

## Continuous versus discrete free Hamiltonian systems

This article has been downloaded from IOPscience. Please scroll down to see the full text article.

2013 J. Phys. A: Math. Theor. 46 335202

(<http://iopscience.iop.org/1751-8121/46/33/335202>)

View [the table of contents for this issue](#), or go to the [journal homepage](#) for more

Download details:

IP Address: 132.248.33.135

The article was downloaded on 02/08/2013 at 01:25

Please note that [terms and conditions apply](#).

# Continuous versus discrete free Hamiltonian systems

**Kurt Bernardo Wolf**

Instituto de Ciencias Físicas, Universidad Nacional Autónoma de México, Av. Universidad s/n, Cuernavaca, Morelos 62251, Mexico

E-mail: [bwolf@fis.unam.mx](mailto:bwolf@fis.unam.mx)

Received 6 June 2013, in final form 11 July 2013

Published 31 July 2013

Online at [stacks.iop.org/JPhysA/46/335202](http://stacks.iop.org/JPhysA/46/335202)

## Abstract

The Euclidean group contains two models of free Hamiltonian evolution: one has a continuous configuration space in which the wavefunctions obey the Helmholtz equation, and require two initial conditions: initial values and initial velocities; the other is based on a discrete position space where the wavefunctions obey a difference equation, and its evolution requires only initial values. Yet the two models are unitarily equivalent. We find that the two initial conditions of the former correspond, according to their parity, with the initial condition of the latter at alternate points, either even or odd.

PACS numbers: 02.20.Qs, 02.30.Ik, 02.60.Lj, 03.65.Aa

(Some figures may appear in colour only in the online journal)

## 1. Introduction: the Euclidean group

A homogeneous and isotropic medium is invariant under the Euclidean group of translations and rotations. We choose two-dimensional media since they are easily visualized and show the essential issues that we present and solve here. We denote the Euclidean (*inhomogeneous special orthogonal*) group in two dimensions by ISO(2) [1]. The Lie algebra ISO(2) that generates this group has three generators, that we denote by  $Q$ ,  $P$ , and  $H$ , whose Lie (commutation) brackets are

$$[H, Q] = -iP, \quad [H, P] = 0, \quad [Q, P] = iH. \quad (1)$$

The first two brackets we can identify with the two Hamilton equations for free systems, which classically are written with Poisson brackets as  $\{h, q\} = -p$  and  $\{h, p\} = 0$ , where  $q$  and  $p$  are position and momentum, and a Hamiltonian function  $h = \frac{1}{2}p^2$  that generates evolution in time. The last bracket in (1) is distinct from the classical Poisson bracket  $\{q, p\} = 1$ .

A complementary interpretation of the Euclidean algebra (1) is suggested by a realization of its generators as first-order differential operators,

$$\begin{aligned} \widehat{P} &= -i\partial_x, & \widehat{Q} &= -i(x\partial_z - z\partial_x), \\ \widehat{H} &= -i\partial_z, & & (x, z) \in \mathbb{R}^2, \end{aligned} \quad (2)$$

where  $P$  and  $H$  generate translations along  $x$ - and  $z$ -axes, while  $Q$  generates rotations in that plane. There are two physical models of free Hamiltonian systems that we can associate with the Euclidean Lie algebra (1), that are determined by its two distinct subalgebra chains

$$\text{iso}(2) \supset \mathfrak{i}_x \ni P, \tag{3}$$

$$\text{iso}(2) \supset \text{so}(2) \ni Q. \tag{4}$$

Since (3) implies that the spectrum  $\Sigma$  of  $\hat{P}$  is continuous while that of  $\hat{Q}$  is discrete, the two chains harbor the continuous and the discrete model respectively, as we shall detail in section 2 for continuous Helmholtz systems, and in section 3 for discrete free systems.

The unitary irreducible representations of the Euclidean group are determined by the eigenvalues  $k^2 \geq 0$  of its second-order invariant operator,

$$P^2 + H^2 = k^2 1, \quad k \in \mathbb{R}, \tag{5}$$

and are further reduced by parity  $\Pi$ , the inverting element in  $\text{IO}(2)$  that can distinguish between  $\pm k$ . Within one  $\text{ISO}(2)$  representation  $k$ , the Lie algebra  $\text{ISO}(2)$  can be realized by

$$P^\circ = k \sin \theta, \quad H^\circ = k \cos \theta, \quad Q^\circ = -i \frac{d}{d\theta}, \tag{6}$$

which are self-adjoint operators in the Hilbert space  $\mathcal{L}^2(\mathbb{S})$  of square-integrable functions over the circle  $\mathbb{S}$ . Their spectra are  $\Sigma(P) = [-k, k] = \Sigma(H)$  and  $\Sigma(Q) = \mathbb{Z}$  (the integers).

The realization (2) in the representation  $k$  turns equation (5) into the Helmholtz equation for waveforms  $\Phi(x, z)$ ,

$$(\partial_x^2 + \partial_z^2)\Phi(x, z) = -k^2\Phi(x, z). \tag{7}$$

If for initial data we are given the waveform at the line *screen*  $z = 0$ , the  $z$ -evolution of  $\Phi(x, z)$  generated by  $H$  requires the specification of *two* initial conditions: the initial form  $\Phi(x) := \Phi(x, z)|_{z=0}$  and the initial  $z$ -derivative ('velocity'),  $\Phi_z(x) := \partial_z\Phi(x, z)|_{z=0}$ .

On the other hand, the waveforms in free discrete systems (6), where the position coordinate ranges over the integers  $x_m \equiv m \in \mathbb{Z}$ , exhibit waveforms  $\phi(m, z)$ , written as  $\phi(z) \equiv \{\phi_m(z)\}_{m \in \mathbb{Z}}$ , only the initial form  $\phi(0)$  is needed to determine  $z$ -evolution. This apparent mismatch will be resolved in section 4 through finding the explicit unitary map between the waveforms in the two models. In section 5 we shall add some conclusions pertaining the use of this result in the description of waveform propagation in planar multimodal waveguides based on the discrete models where position space is a discrete and finite set of points, and where the description of the corresponding phase space is of interest.

## 2. Helmholtz model on the screen and circle

The function domain of the realization of the  $\text{ISO}(2)$  algebra given in (2), restricted to the representation  $k$  by (5), is the space of oscillatory solutions  $\Phi(x, z)$  of the Helmholtz equation (7). This space of functions can be made into a Hilbert space through defining a Euclidean invariant inner product over the line  $x \in \mathbb{R}, z = 0$ , that we will consider as a *screen* where the initial conditions are impressed or measured [2]. For two waveforms  $\Phi(x), \Psi(x)$  and their  $z$ -derivatives  $\Phi_z(x), \Psi_z(x)$ , this inner product is unique and contains a *nonlocal* measure  $\mu_k$  given by

$$(\Phi, \Psi)_{\mathcal{H}_k} := \int_{\mathbb{R}} dx \int_{\mathbb{R}} dx' (\Phi(x)^* \mu'_k(|x-x'|) \Psi(x) + \Phi_z(x)^* \mu_k(|x-x'|) \Psi_z(x)), \tag{8}$$

$$\mu_k(y) := \frac{1}{4} J_0(ky)/k, \quad \mu'_k(y) := k \partial_y \mu_k(y) = \frac{1}{4} J_1(ky)/y, \tag{9}$$

where  $J_n$  are Bessel functions, and boldface  $\Phi(x, z)$  stands for the pair of functions that we may write as a 2-vector  $\begin{pmatrix} \Phi(x, z) \\ \Phi_z(x, z) \end{pmatrix}$ . Euclidean invariance means that the screen line can be translated or rotated to any other line in the  $x$ - $z$  plane without changing the norms and inner products. We thus have the Hilbert spaces  $\mathcal{H}_k$  of Helmholtz waveforms. The measure (9) can be obtained also from the Haar measure of  $ISO(2)$ , or generally  $ISO(N)$  for the  $N$ -dimensional homogeneous media [3]. This measure was used in [4] to find the least-energy approximation by Helmholtz fields to the initial data available from measurements on a finite number of isolated points on a line.

The Helmholtz equation (7) can be written in *evolution form* generated by  $H$  realized as in (2), by a first-order derivative,

$$\check{H}\Phi(x, z) = \partial_z \Phi(x, z), \quad \check{H} := \begin{pmatrix} 0 & 1 \\ -\Delta_k & 0 \end{pmatrix}, \quad \Phi(x, z) := \begin{pmatrix} \Phi(x, z) \\ \Phi_z(x, z) \end{pmatrix}, \quad (10)$$

where  $\Delta_k := \partial_x^2 + k^2$ . The first ‘vector’ component establishes that  $\Phi_z(x, z) = \partial_z \Phi(x, z)$ , and its replacement into the second component,  $-\Delta_k \Phi = \partial_z \Phi_z$ , yields the original Helmholtz equation (7). The other two  $ISO(2)$  generators in this realization are,

$$\check{P} := \begin{pmatrix} -i\partial_x & 0 \\ 0 & -i\partial_x \end{pmatrix}, \quad \check{Q} := \begin{pmatrix} 0 & x \\ -x\Delta_k - \partial_x & 0 \end{pmatrix}. \quad (11)$$

The checked matrix operators (10) and (11) satisfy the same  $ISO(2)$  commutation relations (1) and as the hatted generators in (2).

The two-dimensional inverse Fourier transform of Helmholtz waveforms has support on a circle of radius  $k$ ; this leads to the following *wave transform* [3, 4], which is a unitary map between  $\Phi(x, z) \in \mathcal{H}_k$  and  $\phi^\circ(\theta) \in \mathcal{L}^2(\mathbb{S})$ ,

$$\Phi(x, z) = \sqrt{\frac{k}{2\pi}} \int_{\mathbb{S}} d\theta \phi^\circ(\theta) \exp(ik(x \sin \theta + z \cos \theta)), \quad (12)$$

$$\phi^\circ(\theta) := \frac{\sigma_\theta}{2} \sqrt{\frac{k}{2\pi}} \int_{\mathbb{R}} dx \left( \Phi(x, 0) \cos \theta + \frac{1}{ik} \frac{\partial \Phi(x, z)}{\partial z} \Big|_{z=0} \right) \exp(-ikx \sin \theta). \quad (13)$$

On the circle and in this representation, the  $ISO(2)$  generators (1) are realized by (6).

The  $z$ -evolution by  $\mathcal{T}_z = \exp(izH^\circ)$  of  $\phi^\circ(\theta)$  is thus

$$\mathcal{T}_z \phi^\circ(\theta) = \phi^\circ(\theta, z) = \exp(ikz \cos \theta) \phi^\circ(\theta). \quad (14)$$

From here one derives the  $z$ -evolution of the  $\mathcal{H}_k$  waveforms by a Green function  $G^c(x, x'; z)$  and its  $z$ -derivative,

$$\Phi(x, z) = \int_{\mathbb{R}} dx' \frac{\partial G^c(x, x'; z)}{\partial z} \Phi(x') + \int_{\mathbb{R}} dx' G^c(x, x'; z) \Phi_z(x'), \quad (15)$$

$$G^c(x, x'; z) = G^c(|x-x'|; z) = \frac{1}{4\pi i} \int_{-\pi}^{\pi} d\theta \sigma_\theta \exp(ik(|x-x'| \sin \theta + z \cos \theta)), \quad (16)$$

where  $\sigma_\theta := \text{sign} \cos \theta$ . This continuous Helmholtz model is based on the subalgebra chain (3); its  $z$ -evolution is unitary in  $\mathcal{H}_k$  and, as we stated in the introductory section, it involves separately the initial form and the initial  $z$ -velocity of the Helmholtz waveform at the chosen screen.

### 3. The discrete model and the circle

The discrete model of free systems is also based the Euclidean algebra (1) that incorporates the two Hamilton equations, and also belongs to the irreducible representation  $k$  in (5), but is

distinct from the Helmholtz model of the previous section for being reduced by the subalgebra chain (4) to the compact generator  $Q$ , whose spectrum we understand to be the space of positions in the system driven by the Hamiltonian  $H$ . With  $Q$  represented by diagonal matrix,  $\Sigma(Q) = \mathbb{Z}$ , and using  $H \pm iP$  to raise and lower its eigenvalues, one finds the following representation of  $ISO(2)$  by infinite matrices of elements  $(m, m') \in \mathbb{Z}$ , as given by:

$$\begin{aligned} P_{m,m'} &= -i \frac{1}{2} k (\delta_{m,m'-1} - \delta_{m,m'+1}), & Q_{m,m'} &= m \delta_{m,m'}. \\ H_{m,m'} &= \frac{1}{2} k (\delta_{m,m'-1} + \delta_{m,m'+1}), \end{aligned} \tag{17}$$

These matrices satisfy (5) and are self-adjoint in the Hilbert space of functions  $\boldsymbol{\phi} \in \ell^2(\mathbb{Z})$  of square-summable sequences, i.e., vectors  $\boldsymbol{\phi} = \{\phi_m\}_{m \in \mathbb{Z}}$ , to which we may refer as the *signals* sensed at points on a line: the chosen  $z = 0$  screen.

Hamiltonian evolution along the  $z$ -axis normal to the screen is given as before by the  $ISO(2)$  translation  $\mathcal{T}_z = \exp(izH)$ , which is here represented by a matrix  $\mathbf{G}^d(z)$  acting as a (discrete) Green function,

$$\begin{aligned} \mathcal{T}_z : \boldsymbol{\phi}(0) &= \boldsymbol{\phi}(z), & \phi_m(z) &= \sum_{m' \in \mathbb{Z}} G_{m,m'}^d(z) \phi_{m'}(0), \\ G_{m,m'}^d(z) &= G^d(|m-m'|; z) = e^{i\pi|m-m'|/2} J_{|m-m'|}(kz). \end{aligned} \tag{18}$$

Here the Bessel functions  $J_n(y)$  are of integer orders  $n$ , so  $J_{-n}(y) = J_n(-y) = (-1)^n J_n(y)$ , and thus  $G_{m,m'}^d(-z) = G_{m',m}^d(z)^*$  is unitary in  $\ell^2(\mathbb{Z})$ . As stated in the introductory section, only the initial data  $\boldsymbol{\phi}(0)$  are needed for evolution in the discrete model of free systems.

As indicated in the title to this section, waveforms in the free discrete model outlined above on  $\phi_m \in \ell^2(\mathbb{Z})$ , can be mapped unitarily to waveforms  $\phi^\circ(\theta) \in \mathcal{L}^2(\mathbb{S})$  on the circle, through Fourier series,

$$\phi^\circ(\theta) := \frac{1}{\sqrt{2\pi}} \sum_{m \in \mathbb{Z}} \phi_m \exp(-im\theta), \quad \phi_m = \frac{1}{\sqrt{2\pi}} \int_{\mathbb{S}} d\theta \phi^\circ(\theta) \exp(im\theta). \tag{19}$$

This map also intertwines the realizations of the generators on the integers (17) and on the circle (6).

#### 4. Map between continuous and discrete systems

Both the continuous and discrete free systems have been mapped on the circle. Combining the wave transform (13) with the Fourier series (19), yields

$$\begin{pmatrix} \Phi(x) \\ \Phi_z(x) \end{pmatrix} = \sqrt{k} \sum_{m \in \mathbb{Z}} \phi_m \begin{pmatrix} J_m(kx) \\ imJ_m(kx)/x \end{pmatrix} \tag{20}$$

$$\phi_m = \frac{1}{2\sqrt{k}} \int_{\mathbb{R}} dx (m\Phi(x)/x - i\Phi_z(x)) J_m(kx), \tag{21}$$

which provides a unitary map between the continuous and discrete model waveforms in  $\mathcal{H}_k$  and in  $\ell^2(\mathbb{Z})$  respectively. To verify that (21) is the inverse of (20) we note the integral from [5, 6.538.2],

$$\int_{\mathbb{R}} dx \frac{m}{x} J_m(kx) J_n(kx) = \frac{1}{2} \delta_{m,n}, \tag{22}$$

which is valid for  $m, n > 0$ , but (21) can be continued for  $\phi_0 = 1/\sqrt{2\pi}$  down to  $m = 0$ .

To understand how this map works, we note first that, under inversions, parity  $\sigma \in \{+, -\}$  in the  $m$ -lattice and in the  $x$ -line is preserved:

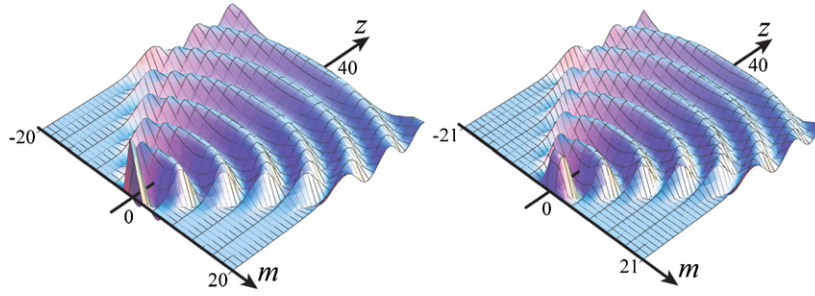


**Figure 1.**  $z$ -evolution in the discrete model of a free system (with  $k = 1$ ). For visibility, we interpolate the discrete  $m$ -points with lines. Left:  $z$ -evolution of an initial unit impulse signal  $\kappa_m(0) := \delta_{m,0}$  (with zero velocity) plotted at even  $m = 2n$  positions  $\kappa_{2n}(z) = (-1)^n J_{2n}(z)$ . Right:  $z$ -evolution of an initial kick  $i\kappa'_m(0) := \frac{1}{2}(\delta_{m,1} + \delta_{m,-1})$  plotted at odd  $m = 2n + 1$  positions,  $i\kappa'_{2n+1}(z) = (-1)^n J_{2n+1}(z)$  that starts from equilibrium.

$$\phi_m = \sigma \phi_{-m} \leftrightarrow \begin{cases} \Phi(x) = \sigma \Phi(-x), \\ \Phi_z(x) = \sigma \Phi_z(-x), \end{cases} \quad (23)$$

due to  $J_{-m}(y) = J_m(-y)$ . And generally for even and odd points  $m$ , (20) leads to

$$\phi_m = \phi_{-m} \leftrightarrow \Phi(x) = 2\phi_m \sqrt{k} \begin{cases} \begin{pmatrix} J_m(kx) \\ 0 \end{pmatrix} & m \text{ even,} \\ i \begin{pmatrix} 0 \\ mJ_m(kx)/x \end{pmatrix} & m \text{ odd,} \end{cases} \quad (24)$$

$$\phi_m = -\phi_{-m} \leftrightarrow \Phi(x) = 2\phi_m \sqrt{k} \begin{cases} i \begin{pmatrix} 0 \\ mJ_m(kx)/x \end{pmatrix} & m \text{ even,} \\ \begin{pmatrix} J_m(kx) \\ 0 \end{pmatrix} & m \text{ odd.} \end{cases} \quad (25)$$

Thus we see that a real symmetric pair  $\phi_m = \phi_{-m}$  at even  $m$  corresponds with the initial form of a real Helmholtz waveform (with no initial velocity,  $\Phi_z(x) = 0$ ), and at odd  $m$  with  $i$  times the initial velocity of the continuous field (starting with zero waveform  $\Phi(x) = 0$ ). The phase of the latter is  $e^{i\pi/2}$  times that of the former, so the waveform indeed advances along the  $z$ -axis. Conversely, a real skew-symmetric pair  $\phi_m = -\phi_{-m}$  at even  $m$  yields  $i$  times initial velocities, and at odd  $m$  real initial forms, so the field moves in the  $-z$ -direction. Stationary Helmholtz fields  $\Phi_z(x) = 0$  correspond to discrete fields that are symmetric ( $\sigma = +1$ ) at even- $m$  points and skew-symmetric ( $\sigma = -1$ ) at odd- $m$  ones.

Further insight into the separate roles played by the even- and odd- $m$  positions is provided by the dynamics of  $z$ -evolution that is illustrated in figure 1. The Green matrix of the discrete model is  $G_{m,m'}^d(z)$  in (18), where we observe that two neighboring waveform values,  $\phi_m(z)$  and  $\phi_{m'}(z)$  with  $|m - m'| = 1$ , are related with a phase of  $e^{i\pi/2}$ . This indicates an alternation between the values and velocities of the discrete waveform in (24)–(25). On the other hand, *second* neighbors with  $|m - m'| = 2$ , are related with a minus sign.

In figure 1 we show the  $z$ -evolution of two initial conditions of even parity,  $\sigma = +$  in (23), as given by (24): the unit impulse  $\kappa_m(0) := \delta_{m,0}$  at the even  $m = 0$  origin and plotted only at the even- $m$  points; and that of a unit kick  $i\kappa'_m(0) := \frac{1}{2}(\delta_{m,1} + \delta_{m,-1})$  plotted only at the odd- $m$  points. These basic discrete waveforms are invariant under displacements by 2 units. The waves in the figure open in beam of half-angle  $\cot \alpha \approx k$  because  $J_m(kz)$  starts to oscillate after  $m \approx kz$ ; the wavenumber  $k$  only changes the scale along the  $z$ -axis. Real initial conditions

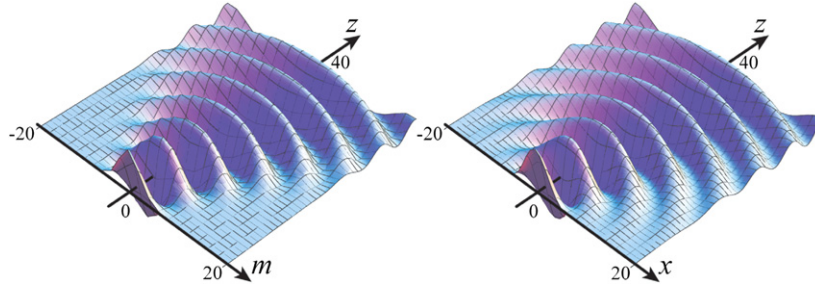


**Figure 2.**  $z$ -evolution of diffused unit-impulse initial values. Left: in the discrete model the signal  $\kappa_{2n}(z) = (-1)^n J_{2n}(z+5i)$  is plotted only at the even  $m = 2n$  positions (interpolated with lines). Right: in the continuous model, the analytic waveform  $K(x, z)$  is  $J_0(k\sqrt{x^2+(z+5i)^2})$ .

$\phi_m(0)$  over even (or odd) positions  $m$  evolve into real discrete waveforms  $\phi_m(z)$  measured on those points. For  $\sigma = -$  functions in (23), the roles of even and odd points  $m$  are exchanged as we can see in (25).

In the discrete case, the unit impulse  $\kappa_m(0)$  is the narrowest waveform in the model; through (20), its corresponding Helmholtz waveform  $K(x) = \sqrt{k} J_0(kx)$  is also the narrowest, but in the  $x$ - $z$  plane it is circularly symmetric:  $K(x, z) = \sqrt{k} J_0(kr)$ , with  $r := \sqrt{(x^2+z^2)}$ . The unit kick  $\kappa'_m(0)$  has a width of 2 units (in  $m$ ) and corresponds to  $K'(x, z) = J_1(kr) e^{\pm i\theta}/r$ , the next-to-narrowest waveform, with a circular phase symmetry. This is the salient difference between the discrete and continuous models of free systems (yet see the next paragraph). In [4] we noted that the central peak of  $J_0(y)$  is narrower than that of  $\text{sinc } y = J_{1/2}(y)/\sqrt{y}$ , which is commonly used for interpolation between equidistant point-values (and which in turn is narrower than that of  $J_1(y)/y$ ); their use for a ‘Helmholtz interpolation’ is thus intrinsically adapted for Helmholtz waveforms and their  $z$ -velocities.

When the evolution parameter  $z$  is allowed to become complex,  $i\zeta$  with  $\zeta$  real, free Hamiltonian systems become diffusive systems [6–8]. Under diffusion, the unit impulse signal  $\kappa_0(m)$  evolving through  $i\zeta$  finds a Green function (18) that is a modified Bessel function  $J_{2m}(e^{i\pi/2}\zeta) = (-1)^m I_{2m}(\zeta)$ , which has a bell shape over the integers—even and odd. For complex  $z+i\zeta$ , its matrix elements on the even integers are  $G_{2m,0}^d(z+i\zeta)$ , shown in figure 2, where they are compared with a continuous complex Bessel–Gauss beam [9],  $J_0(k\sqrt{x^2+(z+i\zeta)^2})$ , which is a Helmholtz solution with null initial velocity. With growing  $\zeta > 0$ , the latter acquires a widening waist at  $z = 0$  while the angle of the beam apron reduces, so at some  $\zeta$  it comes to resemble the discrete diffused solutions, as in the figure. When  $\zeta$  increases, the direction range narrows until it becomes a plane wave.

### 5. Conclusions

We have related the evolution of waveforms in the continuous Helmholtz free Hamiltonian system, with signals in the discrete model. The two models are based on two inequivalent subalgebra reductions of the Euclidean algebra  $ISO(2)$ , the first with respect to the noncompact generator  $P$  of momentum, and the second with respect to the compact position operator  $Q$ , both belonging to the same self-adjoint irreducible representation of the algebra  $k$ . Position space in the Helmholtz model is a double continuum for initial waveforms and velocities; in the second it is the set of integers. We could obviously expect the relation to be a unitary transformation between the  $\mathcal{H}_k$  and  $\ell^2(\mathbb{Z})$  Hilbert spaces, but we found a rather subtle correspondence between

a continuous waveform and its  $z$ -velocity, with the odd and even points of a discrete signal, which is determined by the parity of the functions and the parity of the position points.

We should briefly comment on the *Schrödinger* free system, whose Hamiltonian is  $H^{\text{Sch}} = \frac{1}{2}(P^{\text{Sch}})^2$ , with the quantum operators of position  $Q^{\text{Sch}} = q \cdot$  and momentum  $P^{\text{Sch}} = -i\partial_q$ , which close into a four-parameter algebra with  $[Q^{\text{Sch}}, P^{\text{Sch}}] = i1$ . Under commutation, these operators close into a Lie algebra which is *not* ISO(2), and which does not have a compact generator to serve as position operator in a discrete model. Instead, free evolution is given by the  $z$ -dependent Fresnel transform. In the free quantum system, the evolution of a centered Gaussian,  $\zeta$ -diffused out of a Dirac  $\delta$ , is  $\sim \exp[-x^2/2(\zeta + iz)]/(\zeta + iz)$ , which bears little resemblance to the evolution of the continuous or discrete systems based on ISO(2).

Other discrete Hamiltonian models whose evolution generator is represented by a tri-diagonal matrix with zeros on the main diagonal, as  $P$  or  $H$  here, or their sums, products and powers, will also dynamically relate the waveform values  $\phi_m$  at even- $m$  points only among themselves, and odd points only. Such Hamiltonians have been used to treat multimodal waveguide systems, harmonic but with aberrations, represented by unitary evolution matrices. When eigenvectors are demanded from a computer—the ground state for example—the result can be a ‘Gaussian porcupine’ whose odd points are all zero [10]. Tying together separately even and odd points can provide a better understanding of such discrete systems and their relation to a continuous counterpart system that obeys the same algebra.

## Acknowledgments

I thank N M Atakishiyev, J Rueda-Paz, and J C Gutiérrez-Vega for their interest in this work and helpful comments, and Guillermo Krötzsch for producing the figures. Support for this research has been provided by the *Óptica Matemática* projects by UNAM (PAPIIT IN101011) and by the National Council for Science and Technology (SEP-CONACYT 79899).

## References

- [1] Gilmore R 1974 *Lie Groups, Lie Algebras, and Some of Their Applications* (New York: Wiley)
- [2] Steinberg S and Wolf K B 1981 Invariant inner products on spaces of solutions of the Klein–Gordon and Helmholtz equations *J. Math. Phys.* **22** 1660–3
- [3] Wolf K B 1989 Elements of Euclidean optics *Lie Methods in Optics (Lecture Notes in Physics vol 352)* (Heidelberg: Springer) chapter 6, pp 115–62
- [4] González-Casanova P and Wolf K B 1995 Interpolation of solutions to the Helmholtz equation *Numer. Methods Partial Differ. Eqns* **11** 77–91
- [5] Gradshteyn I S and Ryzhik I M 2000 *Table of Integrals, Series, and Products* 6th edn, ed A Jeffrey (New York: Academic)
- [6] Deschamps G A 1971 The Gaussian beam as a bundle of complex rays *Electron. Lett.* **7** 684
- [7] Arnaud J 1985 Representation of Gaussian beams by complex rays *Appl. Opt.* **24** 538–43
- [8] Porras M A, Borghi R and Santarsiero M 2001 Relationship between elegant Laguerre–Gauss and Bessel–Gauss beams *J. Opt. Soc. Am. A* **18** 177–84
- [9] April A 2011 Bessel–Gauss beams as rigorous solutions of the Helmholtz equation *J. Opt. Soc. Am. A* **28** 2100–7
- [10] Rueda-Paz J and Wolf K B 2011 Finite signals in planar waveguides *J. Opt. Soc. Am. A* **28** 641–50